The Journal of Experimental Biology 213, 4272-4277

doi:10.1242/jeb.049320

Mechanics and kinematics of backward burrowing by the polychaete *Cirriformia moorei*

James Che and Kelly M. Dorgan*

University of California, Berkeley, Department of Integrative Biology, 3060 VLSB No. 3140, Berkeley, CA 94720, USA

*Author for correspondence (kelly.dorgan@berkeley.edu)

Accepted 25 September 2010

SUMMARY

The polychaete *Cirriformia moorei* burrows in muddy sediments by fracture, using its hydrostatic skeleton to expand its anterior region and exert force against its burrow wall to extend a crack. Burrowing occurs in four phases: stretching forward into the burrow, extending the crack anteriorly, thickening the burrowing end to amplify stress at the tip of the crack, and bringing the rest of the body forward as a peristaltic wave travels posteriorly. Here, we show that *C. moorei* is also able to burrow with its posterior end using a similar mechanism of crack propagation and exhibiting the same four phases of burrowing. Worms burrowed backwards with similar speeds and stress intensity factors as forward burrowing, but were thinner and less blunt and did not slip as far away from the crack tip between cycles of burrowing. The anterior end is more muscular and rigid, and differences in body shapes are consistent with having reduced musculature to dilate the posterior segments while burrowing. Backward burrowing provides a unique opportunity to study the effects of morphology on burrowing mechanics within the same species under identical conditions.

Supplementary material available online at http://jeb.biologists.org/cgi/content/full/213/24/4272/DC1

Key words: sediment mechanics, burrowing, biomechanics, fracture, locomotion, peristalsis, hydrostatic skeleton, gelatin, Cirratulidae, *Cirriformia moorei.*

INTRODUCTION

Marine burrowers move through muddy sediments by extending crack-shaped burrows by fracture (Dorgan et al., 2005). Burrowing infauna contribute to the cycling of organic carbon and alter the composition of the sediment, greatly impacting marine ecosystems through bioturbation (Meysman et al., 2006). Burrowing behavior and kinematics depend on the mechanical properties of the sediment, specifically the stiffness and the fracture toughness. For example, *Nereis virens* Sars everts its pharynx, amplifying stress at the tip of its crack-shaped burrow to overcome high sediment toughness. When burrowing in a medium with higher stiffness relative to toughness, *N. virens* instead moves its head from side to side in its burrow to drive itself forward like a wedge, and extends the crack edges laterally to reduce compression on its body from the elastic material (Dorgan et al., 2008). Behavior and kinematics also depend on the size of the organism; smaller worms are relatively thicker and blunter than larger worms and exhibit a greater variation in thickness over a burrowing cycle (Che and Dorgan, 2010). These differences are consistent with predictions from fracture mechanics theory and reflect the means to increase the stress amplified at the crack tip so that the stress intensity factor (K_I) reaches the critical stress intensity factor (K_{Ic}), or fracture toughness, a material property that varies considerably in sediments (Johnson et al., 2002; Dorgan et al., 2008). Burrow extension by fracture occurs when K_I exceeds K_{Ic}.

Observations of burrowing behavior have been impeded by the difficulty in visualizing organisms in substrata, but an emerging technique involves the use of gelatin in seawater as a mechanical analog for muddy sediments (Johnson et al., 2002; Dorgan et al., 2005; Boudreau et al., 2005). Analyses of mechanics and kinematics have been carried out for the nereid *N. virens* (Dorgan et al., 2007; Dorgan et al., 2008), the cirratulid *Cirriformia moorei* Blake 1996 (Che and Dorgan, 2010), and the glycerid *Hemipodus simplex* Grube 1857 (E. A. K. Murphy and K.M.D., unpublished). Muddy sediments, like gelatin, are elastic solids, and the two media have similar mechanical properties and therefore similar fracture behavior (Johnson et al., 2002; Boudreau et al., 2005). Observations of crack growth in gelatin are thus representative of those in muddy sediments, and this medium is appropriate for studying the mechanics of burrowing during relatively short time periods. Gelatin might be less appropriate for studies of burrowing behavior over longer time periods, as, unlike sediment, gelatin shows no loss of elastic stored energy (Dorgan et al., 2007).

Cirriformia moorei is an abundant marine polychaete in intertidal mudflats, and Cirratulidae are common globally in shallow environments, as well as in the deep sea (see Rouse and Pleijel, 2001). We have recently shown that *C. moorei* burrows by crack propagation, using its hydrostatic skeleton to exert a dorso-ventral force against the walls of the burrow to extend a crack and move the body forward (Che and Dorgan, 2010). The worms exhibit four distinct burrowing phases to move through sediment (Che and Dorgan, 2010). In the forward stretching phase, the anterior of the worm elongates towards the tip of the crack. Next, the anterior crack extension phase begins as the worm thickens slightly and continues moving forward, while extending the crack to the maximum distance traveled for the burrowing cycle. The anterior body thickening phase occurs after the maximum distance is achieved; the anterior end thickens to its maximum, causing the dorso-ventral stress to be amplified at the tip of the crack so that it extends laterally. Finally, the cycle ends with a peristaltic wave progression phase, in which the rest of the body is brought forward into the crack by peristalsis.

While studying size effects on burrowing behavior, we found that *C. moorei* is also able to burrow backward with its posterior end. *Cirriformia moorei* is distinctly different morphologically in its anterior and posterior ends: the anterior end contains many branchial filaments, whereas the posterior end has few or none; and the anterior appears more muscular and has a mouth and buccal organs that are likely to increase rigidity (Fig. 1). Here, we present data on the mechanics and kinematics of backward burrowing, compare our findings with those from forward-burrowing worms, and discuss the relationship between morphology and burrowing mechanics in the same animal.

MATERIALS AND METHODS

Animals

The cirratulid polychaetes, *Cirriformia moorei* (0.01–0.68 g wet mass), were collected from Doran Regional Park, Bodega Bay, CA, USA, and Inverness, Tomales Bay, CA, USA, during low tide, and were kept at 11°C in containers of mud with aerated seawater until use.

Experimental setup

The experimental setup was the same as that used by Che and Dorgan (Che and Dorgan, 2010). Experiments were conducted in a cold room at 11°C. A clear, glass tank of gelatin was placed in front of a Porta-Trace (Gagne, Inc., Johnson City, NY, USA) light table that provided background lighting for the CCD video camera (Basler A622f, Exton, PA, USA) connected to a PC. Gelatin (www.bulkfoods.com) was boiled at high concentration with artificial seawater (Instant Ocean, Aquarium Systems, Inc., Mentor, OH, USA). Additional artificial seawater was then added to dilute the solution and obtain the appropriate concentration (28.35 g liter seawater^{-1}). The containers of gelatin were left to set overnight in a refrigerator before use.

Worms were coerced to burrow with their posterior ends by making a small crack on the surface of the gelatin with forceps, inserting the worm into the crack, and orienting the posterior end towards the bottom edge of the crack. Video footage of *C. moorei* was recorded for both dorsal and lateral views in the same manner as that described by Che and Dorgan (Che and Dorgan, 2010), with the video camera run by LabView software (version 7.1.1, National Instruments, Austin, TX, USA) at 3.75 frames s^{-1} (fps). Usable segments of video included at least four burrowing cycles in which the worm did not stop, change direction, move out of the field of view of the video camera, or come within 0.015 m of the tank wall. Worms that burrowed favorably were preserved in formalin and later measured for weight, length, and width and thickness at the fourth and eighth setigers.

Data analysis

From the recorded videos (supplementary material Movies 1 and 2), contours around the body of the worm in both dorsal and lateral view were determined using ProAnalyst (Xcitex, Inc., Cambridge, MA, USA) and used to calculate body widths and thicknesses, respectively. The coordinates from each point along the contour were exported into Excel (Microsoft, Redmond, WA, USA). Matlab (R2007a, The MathWorks, Inc., Natick, MA, USA) was then used to calculate body thicknesses from the lateral view contours, using the methods of Che and Dorgan (Che and Dorgan, 2010). For forward-burrowing worms, branchial filaments near the anterior region of the body interfered with automated contour measurements of body width; instead width was measured manually at ≥10 distances away from the head for each frame. Branchial filaments are present only at the anterior ends of cirratulids, however, so the contours of dorsal views could be used to calculate body widths of the posterior end during backward burrowing.

Stress intensity factor (K_I) and the distance from the crack tip to the point of contact between the worm body and crack wall (a) were calculated from the thickness profiles (see lateral view; Fig. 1A,C). The computation, described in detail by Dorgan et al. (Dorgan et al., 2008) and Che and Dorgan (Che and Dorgan, 2010), involves simultaneously solving two equations that describe the stress intensity of a wedge with an arbitrary shape, $f(z–b)$, corresponding to the shape of the worm in lateral view (see Fig. 1A,C):

$$K_I = \frac{E\sqrt{2a}}{2\sqrt{\pi}\,(1-\nu)^2}\int_a^\infty \frac{f'(z-b)}{\sqrt{z(z-a)}}\,dz,\quad a > b \quad \text{(Sih, 1973)}, \quad (1)$$

$$K_I = \frac{E}{\sqrt{2\pi a}(1-\nu^2)}\left(h - \int_a^\infty f'(z-b)\sqrt{\frac{z-a}{z}}\,dz\right)$$

(Barenblatt, 1962). (2)

Because neither K_I nor a could be directly measured from the movie data, the two variables were solved by iteratively increasing a until the two K_I values from Eqns 1 and 2 were within a tolerance of 2 Pa m$^{0.5}$. The stress intensity depends on the elastic modulus, E (Pa), and Poisson's ratio, ν (dimensionless), which are both intrinsic properties of the medium describing stiffness and compressibility, respectively. For gelatin, E=7100 Pa and ν=0.45 (Dorgan et al., 2008). In addition, stress intensity depends on the shape and placement of the wedge. The value b (m) is the distance from the tip of the wedge (the end of the worm) to the crack tip, which is assumed to be at the maximum distance that the end of the worm has traveled. The function $f(z–b)$ describes the shape of the wedge, which we model as the half-thickness along the length of the worm (the z-axis), measured from the lateral view of the worm (shown in Fig. 1A,C). The slope of the worm, $f'(z–b)$, describes the bluntness of the worm as it burrows and is calculated from thickness profiles.

In addition to the thickness profiles used to calculate stress intensity factors, dorsal-view videos were analyzed to quantify changes in width profiles over burrowing cycles. For both views, slopes of the profiles, distance traveled over time, mean speed, and the distance that the burrowing end slips away from the crack tip during the peristaltic wave progression phase were calculated using Matlab.

Comparisons with anterior burrowing

Stress intensity factors, slopes, speeds, displacements, minimum values for a, and normalized maximum thicknesses and widths at the burrowing end for backward-burrowing worms were compared with data for forward-burrowing worms from previous experiments in which the same methods were used (Che and Dorgan, 2010). Data were acquired for worms of similar sizes, with a mean width at the eighth setiger of 2.34±0.52 mm and 2.80±0.93 mm for worms that burrowed forwards and backwards, respectively (ANOVA P-value=0.088). The minimum value of a (a_{min}) is the closest distance away from the crack tip that the worm contacts the crack wall and is coincident with the peak in stress intensity factor (Che and Dorgan, 2010). The closer the contact to the crack tip, the more stress is applied to the crack wall and amplified at the crack tip: from Eqns 1 and 2, K_I is inversely proportional to a. Maximum thicknesses were measured at this point in each cycle (at a_{min}). Thicknesses and values of a were normalized for body size by dividing the parameters by measured

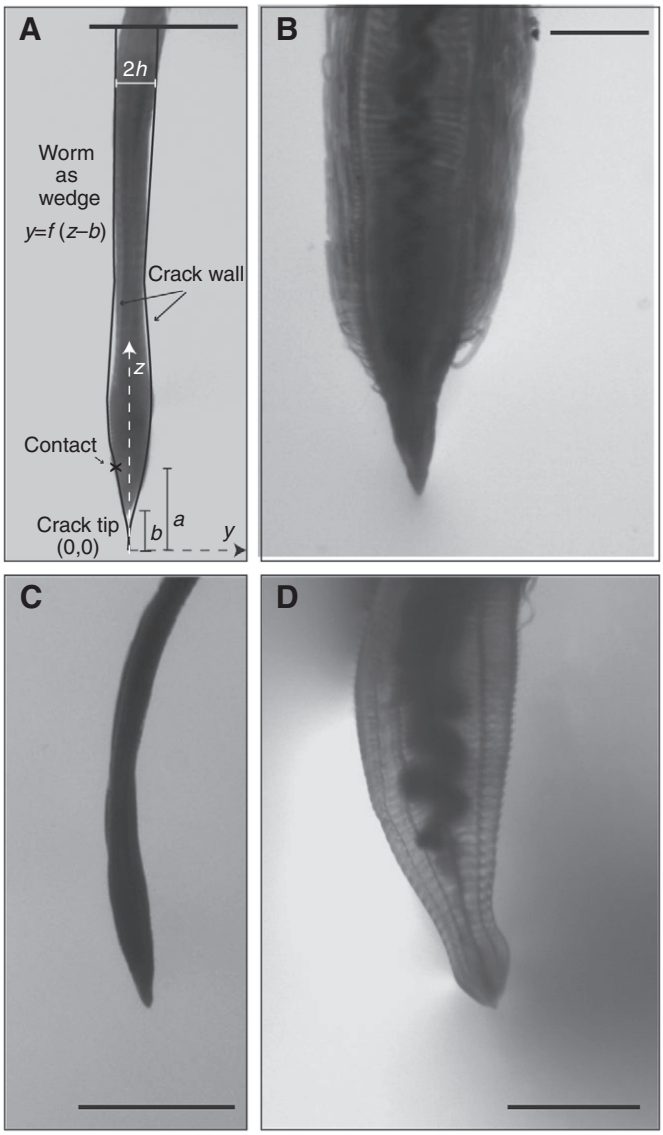

Fig. 1. Lateral (A) and dorsal (B) views of *Cirriformia moorei* burrowing forwards (0.05 and 0.48 g, respectively). Compare with lateral (C) and dorsal (D) views of worms burrowing backwards (0.47 and 0.34 g, respectively). A scheme of the crack is drawn around the worm (A), with worm shape [$f(z-b)$] and distances between the crack tip and the anterior of the wedge (b), and the crack tip and contact of the worm (a), indicated. Scale bars in all images: 2 mm.

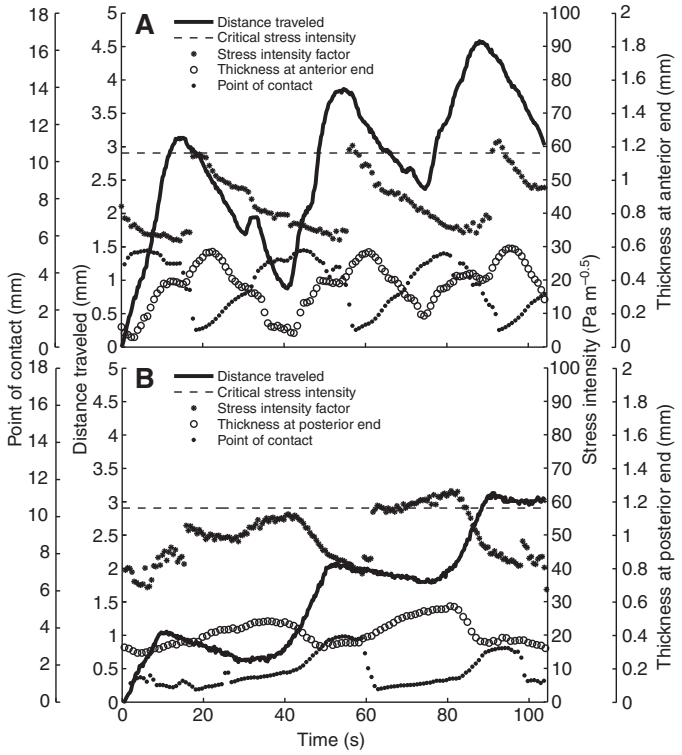

Fig. 2. Distance traveled over time with corresponding stress intensity factors, thickness at the burrowing end and the point of contact between the burrowing end and the crack wall for (A) forward- (0.44 g) and (B) backward-burrowing (0.44 g) *Cirriformia moorei*. Stress intensity is large when thickness at the burrowing end is large and the point of contact is small. For both forward and backward burrowing, peaks in stress intensity occur after the worm reaches the maximum distance traveled for the cycle.

widths of the worms that were preserved in formalin. ANOVA tests were performed using the Analysis ToolPak in Microsoft Excel. In addition, width and thickness profiles were generated in Matlab from both forward and backward burrowers to observe the changes in body shape over the course of the burrowing cycles.

RESULTS

Similar to worms that burrow forwards, backward-burrowing worms exhibited discrete cycles of positive distance traveled followed by a small negative distance traveled, although compared with forward-burrowing worms the distance moved away from the crack tip was smaller (Fig. 2; supplementary material Movies 1 and 2). For both forward and backward burrowing, K_I increased sharply after the worm reached the maximum distance traveled, and this increase was driven by a sharp decrease in a (see Eqns 1 and 2). For forward-burrowing worms, thickness peaked shortly after, then decreased as the point of contact moved away from the crack tip, resulting in a drop in K_I as the worm moved away from the crack tip. For backward burrowing-worms, thickness instead increased slowly until the worm started to extend the crack again, and K_I remained high and a low over this duration. By contrast, the anterior end thickened in two distinct phases during forward burrowing, before and after crack extension, with thickness, a and K_I remaining constant as the crack grew.

For both forward- and backward-burrowing worms, thickness at the burrowing end was relatively small as the worm stretched forward and into the crack (Fig. 3, blue lines) but began to increase after the worm reached the maximum distance traveled (Fig. 3, red lines). This dilated region applies stress to the burrow walls and also serves to initiate peristaltic waves, which travel from the burrowing end down the length of the body. The slope of the wedge or the worm's body, $f'(z-b)$, was largest near the burrowing end of the worm, and decreased towards zero further along the body for both dorsal and lateral profiles of forward- and backward-burrowing worms, as expected (Fig. 3C,F). For both forward and backward burrowers, the slope was lower near the burrowing end while the worm was extending the crack (blue) than either before the worm stretched toward the crack tip (green) or once the worm expanded the burrowing end after it reached the maximum distance traveled for the cycle (red), although these differences occurred closer to the

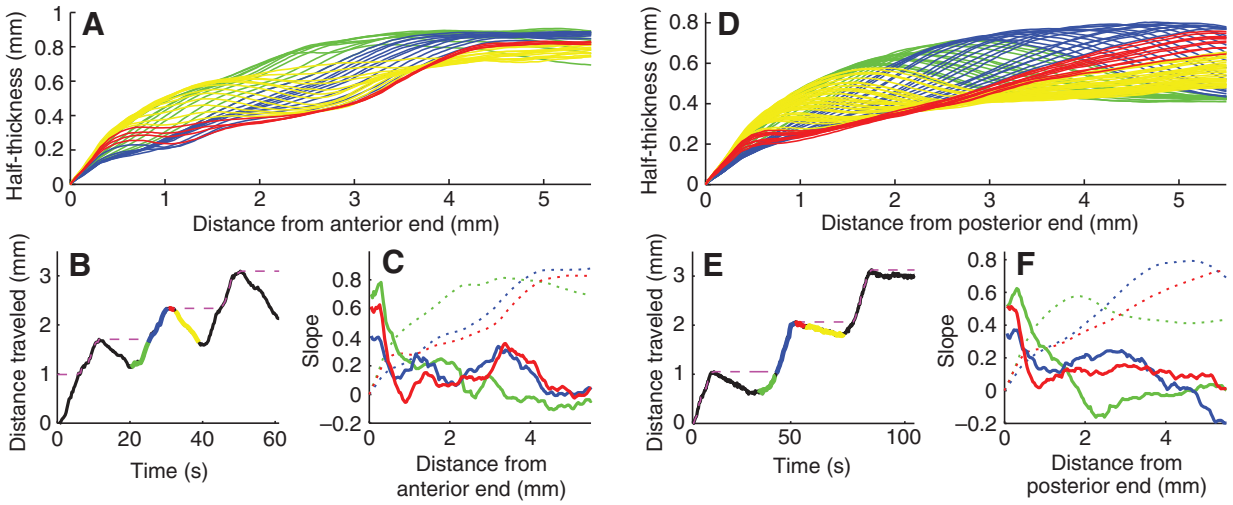

Fig. 3. Thickness profiles for forward- (A, 0.38 g) and backward-burrowing (D, 0.44 g) *Cirriformia moorei*, with corresponding distance traveled (B,E) and slope along the length of the body (C,F). Slopes are shown for one selected thickness profile in each phase, which is shown as a dotted line in the same color. In both cases, worms exhibit four phases in each cycle of burrowing, in which the burrowing end moves towards the crack tip (green), pushes into and extends the crack (blue), thickens after reaching the maximum distance traveled (red), and pulls the rest of the body forward by peristalsis (yellow).

crack tip than did the contact of the worm with the burrow wall (black dots) so did not affect K_I. Widths showed similar patterns to thicknesses (Fig. 4), and this synchrony results from the peristaltic wave traveling along the worm during each cycle.

Compared with worms burrowing forwards, the distance that worms slipped away from the crack was significantly smaller for backward burrowers (Table 1). In addition, the point of contact of the worm with the burrow wall was closer to the tip of the crack for backward-burrowing worms, and at the point of contact the maximum thickness and the slope were significantly smaller. Maximum stress intensity values and mean speeds were not significantly different for worms burrowing with either end.

DISCUSSION

Although the mechanics and kinematics are very similar, backward-burrowing worms exhibit a few differences in thickness and stress-intensity cycles when compared with forward-burrowing worms, most notably that backward-burrowing worms slip away from the crack tip less between burrowing cycles. Upon examination of dorsal and lateral videos, it appears that dilation in forward-burrowing worms is achieved with a direct and localized dorso-ventral expansion caused by longitudinal muscle contraction, whereas this dilation is less localized for backward-burrowing worms. Expansion of the end of the tail might be achieved by moving the posterior region of the worm forward into the crack tip and using fracture

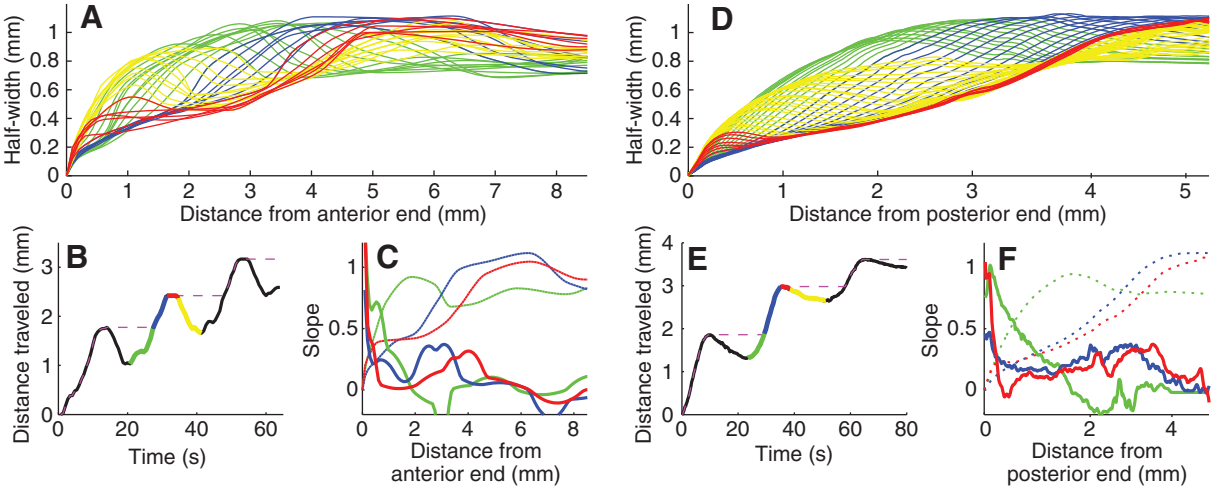

Fig. 4. Width profiles for forward (A, 0.09 g) and backward (D, 0.12 g) burrowing *Cirriformia moorei*, with corresponding distance traveled (B,E) and slope along the length of the body (C,F). Slopes are shown for one selected width profile in each phase, which is shown as a dotted line in the same color. Because fewer width measurements were used to obtain the profile of the forward-burrowing worm, it appears less smooth (see Materials and methods). Changes in widths are similar to changes in thickness (Fig. 3), in which both the anterior and posterior ends become relatively thin as the burrowing end moves towards the crack tip (green), remain thin as the end is pushed into the crack (blue), widen after reaching the maximum distance traveled (red) and exhibit peristaltic wave progression (yellow).

Table 1. ANOVA statistics for comparisons of displacement, point of contact with the burrow wall (a_{min}), slope, thickness, width, speed and stress intensity factors between forward- and backward-burrowing *Cirriformia moorei*

Parameter	Forward	Backward	*P*
Reverse displacement (mm)	0.75±0.32	0.39±0.17	0.0067*
Normalized a_{min}	0.13±0.01	0.065±0.013	0.016*
Maximum slope near tip	0.47±0.12	0.31±0.04	0.0042*
Normalized maximum thickness at a_{min}	0.12±0.01	0.042±0.007	6.86×10^{-5}*
Normalized maximum thickness at $a_{min,avg}$	0.11±0.008	0.060±0.010	0.0017*
Normalized maximum width at $a_{min,avg}$	0.12±0.024	0.077±0.014	0.53
Mean speed (mm s^{-1})	0.048±0.027	0.059±0.047	0.44
Maximum stress intensity (Pa $m^{0.5}$)	55.82±10.09	56.29±10.33	0.92

Comparisons for thickness and width were made at the mean value of a_{min} (0.21±0.015 mm) for forward and backward burrowers. The mean values of a_{min} were calculated from thickness data and could not be calculated for width measurements. Thickness was normalized by dividing the maximum thickness by the measured preserved width of the worm after it was preserved in formalin. The comparisons were performed for 21 worms that burrowed forwards (2.34±0.52 mm at the eighth setiger) and eight worms that burrowed backwards (2.80±0.93 mm at the eighth setiger), for a total of 29 worms (except for normalized width at mean a_{min}, in which three backward- and six forward-burrowing worms were used). ANOVA tests with a *P*-value of <0.05 were considered significant, as indicated by the asterisks.

resistance to complement muscle contraction. Although we did not specifically examine muscle structure at the two ends, transparency of the posterior (Fig. 1D) is a clear indication of poorer muscularization of the posterior. Movement of body mass towards the crack tip would enable the worm to expand with less localized muscle power, and accounts for the relatively small displacement away from the crack tip and the lengthy duration of thickening (Fig. 2).

Peristaltic wave progression occurs along the length of the worm when the dilated region at the burrowing end begins traveling away from the crack tip. For worms burrowing with the posterior end, peristaltic progression partially overlaps with the forward-stretching phase of the next cycle, whereas it appears as a distinctly separate phase in forward-burrowing worms before forward stretching occurs. This can be seen as a reduction in slipping away from the crack tip in the plot of distance traveled for backward-burrowing worms (Fig. 2). As the peristaltic wave moves away from the crack tip, the burrow walls recoil elastically to compress the tip of the worm. The anterior end of the worm contains the buccal cavity, ganglia and sensory organs, and appears more muscular, whereas the posterior has less structure and likely changes shape more easily. Compared with the head, the tail is thinner and more pointed (Table 1). Although worms burrowing forwards are relatively thicker than backward burrowers, worms that burrow with the posterior end are able to make contact with the crack wall closer to the crack tip, thus achieving similar stress intensity factors. Movement away from the crack tip might prevent the head from being compressed during forward burrowing, whereas compression of the tail increases surface contact and could hold the end in place while the rest of the body moves into the crack. Alternatively, the slipping of the anterior end might be an effect of longitudinal muscle contraction to expand the body, extend the crack laterally and begin the peristaltic wave; these hypotheses are not mutually exclusive.

For forward and backward burrowing, the peak in K_I occurs after the maximum distance has been traveled, not while the crack extends as predicted from fracture mechanics theory. We explained the low K_I during crack extension by forward-burrowing worms as an artefact of using a 2-D equation for K_I that assumes constant stresses along the width of the worm (Che and Dorgan, 2010). The extending crack is much narrower than the body at the point of contact (Figs 3, 4), enabling the worm to focus stress more effectively than is predicted by Eqns 1 and 2. The peak in K_I is likely to correspond with lateral crack extension, when the point of contact with the burrow wall moves closer to the crack tip (Fig. 2, Fig. 3C,F) and the worm becomes thicker (Fig. 3) and wider (Fig. 4). This same pattern occurs for backward burrowing, which suggests a similar separation of anterior and lateral crack extension. The gradual increase in thickness for backward burrowers coinciding with high K_I (Fig. 2) suggests that this lateral crack extension takes longer, which is consistent with the smaller thickness and reduced musculature of the posterior end.

Although there are clear kinematic differences between forward and backward burrowing, the general mechanics are very similar. *Cirriformia moorei* uses its hydrostatic skeleton for burrow extension and locomotion in both forward and backward burrowing. In both cases, burrow extension is achieved by exerting dorso-ventral forces against the walls of the crack, and retrograde peristalsis is used to bring the body into the burrow. Moreover, both ends when burrowing exhibited the same four phases, which involve stretching toward the crack tip, pushing into the burrow to further extend the crack, widening the burrowing end to amplify stress at the crack tip, and using a peristaltic wave to bring the rest of the body into the burrow (Fig. 5).

The discovery of backward burrowing introduces a new behavioral factor to consider for locomotion in sediments, but further research is needed to determine how often and under what conditions worms burrow backwards in the natural environment. During experiments, *C. moorei* tended to burrow for noticeably shorter periods with the posterior end, and the worms would continue only if agitated with a pipette tip. Also, worms changed direction frequently as they burrowed backwards. By contrast, worms that burrowed forwards typically exhibited a consistent, steady pace of locomotion in a single direction for longer periods. It might be that in the field worms burrow forwards when moving any considerable distance and use backward burrowing for short escape responses and maneuvering over small distances. Cirratulids are typically oriented with the anterior end closer to the surface of the sediment with branchial filaments splayed on the surface or near the sediment-water interface (Ronan, 1977; Shull and Yasuda, 2001) (K.M.D. and J.C., unpublished).

Our observations raise questions about whether backward-burrowing behavior occurs for other species in the Cirratulidae family, as well as for other polychaetes. The ability to burrow backwards might be advantageous in escaping from epibenthic predators, might enable the worms to keep their gills closer to the

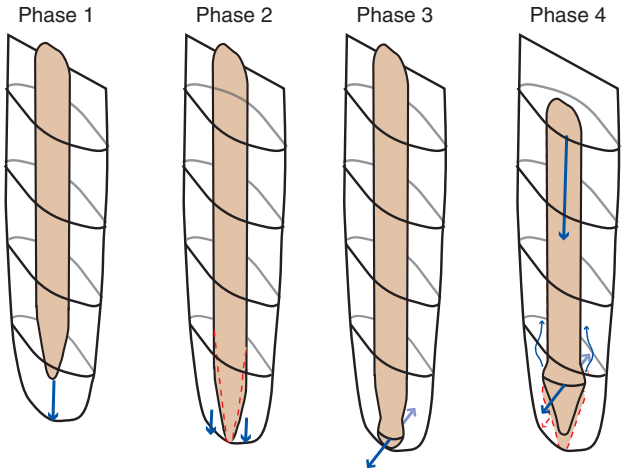

Fig. 5. Diagram of the four key phases of burrowing. In each cycle, *Cirriformia moorei*: (1) stretches the burrowing end towards the crack tip; (2) pushes into and extends the crack; (3) thickens the burrowing end to exert dorso-ventral forces on the burrow walls, amplifying stress at the crack tip; and (4) uses a peristaltic wave to bring the rest of the body forward into the burrow. Backward burrowing differs from forward burrowing (red dotted lines) in phase 2, in which it is more pointed as it stretches forward, and in phase 4, in which it does not slip as far back away from the crack tip during the peristaltic wave progression phase.

sediment-water interface by alternating between backward and forward burrowing, and probably provides a maneuverability advantage. Jumars et al. suggest an analogy between long, skinny worms and railroad trains that also carry two locomotives, one at either end; pushing a long worm, like pushing a long train, backwards might be a losing proposition (Jumars et al., 2007). Our research extended to neither the ecological implications of the backward-burrowing mechanism nor its effects on particle mixing. That the mechanics and kinematics of burrowing backwards and forwards are so similar, however, is remarkable. Differences are consistent with the anatomical differences between the two ends, that the anterior is more muscular and rigid to accommodate internal sensory organs.

LIST OF SYMBOLS AND ABBREVIATIONS

a	distance from the tip of the crack to the point of contact between the burrowing end of the worm and the crack wall
a_{min}	mean minimum value of a achieved for each cycle of burrowing
b	distance between the burrowing end of the worm and the tip of the crack
E	modulus of elasticity (Pa)
h	half-thickness of a worm at a point far away from the burrowing end
K_I	stress intensity factor ($Pa\,m^{0.5}$)
K_{Ic}	critical stress intensity factor, fracture toughness ($Pa\,m^{0.5}$)
z	distance from the burrowing end of the worm
ν	Poisson's ratio (dimensionless)

ACKNOWLEDGEMENTS

We thank P. A. Jumars and M. A. R. Koehl for helpful comments on the manuscript. This project was funded by NSF IOS grant #0642249 to M. A. R. Koehl, as well as the Virginia G. and Robert E. Gill Chair to M. A. R. Koehl and the Undergraduate Research Apprenticeship Program, University of California, Berkeley.

REFERENCES

Barenblatt, G. (1962). The mathematical theory of equilibrium cracks in brittle fracture. *Adv. Appl. Mech.* **7**, 55-129.
Boudreau, B. P., Algar, C., Johnson, B. D., Croudace, I., Reed, A., Furukawa, Y., Dorgan, K. M., Jumars, P. A., Grader, A. S. and Gardiner, B. S. (2005). Bubble growth and rise in soft sediments. *Geology* **33**, 517-520.
Che, J. and Dorgan, K. M. (2010). It's tough to be small: dependence of burrowing kinematics on body size. *J. Exp. Biol.* **213**, 1241-1250.
Dorgan, K. M., Jumars, P. A., Johnson, B., Boudreau, B. P. and Landis, E. (2005). Burrowing mechanics: burrow extension by crack propagation. *Nature* **433**, 475.
Dorgan, K. M., Arwade, S. R. and Jumars, P. A. (2007). Burrowing in marine muds by crack propagation: kinematics and forces. *J. Exp. Biol.* **210**, 4198-4212.
Dorgan, K. M., Arwade, S. R. and Jumars, P. A. (2008). Worms as wedges: effects of sediment mechanics on burrowing behavior. *J. Mar. Res.* **66**, 219-254.
Johnson, B. D., Boudreau, B. P., Gardiner, B. S. and Maass, R. (2002). Mechanical response of sediments to bubble growth. *Mar. Geol.* **187**, 347-364.
Jumars, P. A., Dorgan, K. M., Mayer, L. M., Boudreau, B. P. and Johnson, B. D. (2007). Physical constraints on infaunal lifestyles: may the persistent and strong forces be with you. In *Trace Fossils: Concepts, Problems, Prospects* (ed. W. Miller, III), pp. 442-457. Oxford, Amsterdam: Elsevier.
Meysman, F. J., Middelburg, J. J. and Heip, C. H. (2006). Bioturbation: a fresh look at Darwin's last idea. *Trends Ecol. Evol.* **21**, 688-695.
Ronan, T., Jr (1977). Formation and paleontologic recognition of structures caused by marine annelids. *Paleobiology* **3**, 389-403.
Rouse, G. and Pleijel, F. (2001). *Polychaetes*. New York: Oxford University Press.
Shull, D. and Yasuda, M. (2001). Size-selective downward particle transport by cirratulid polychaetes. *J. Mar. Res.* **59**, 453-473.
Sih, G. (1973). *Handbook of Stress-Intensity Factors*. Bethlehem, PA: Lehigh University.